CHAPTER 5

ANALYSIS OF FIBRE PROPERTIES

5.1 Mechanical Property Testing [38, 39]

A fibre must be sufficiently strong to withstand processing by available textile machinery and provide the desired durability in its end-use. The strength of a specimen subjected to tension load is usually reported when fibre properties are compared.

5.1.1 Stress-Strain Behavior

The stress-strain behavior of fibres measured at a constant rate of loading provides a basis for their quality control and comparative evaluation. The diagram shown in Figure 5.1 is typical of that obtained in tension for a constant rate of loading. For compression and shear, the behavior is quite similar except that the magnitude and the extent to which the curve is followed are different.

In the diagram in Figure 5.1, load is plotted against extension. Even for different materials, the nature of the curves will be similar but they will differ in (1) the numerical values obtained and (2) how far the course of the typical curve is followed before failure occurs.

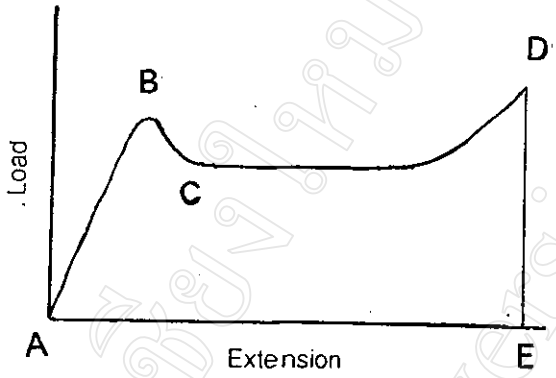

Figure 5.1: A typical stress-strain curve for a drawn polymer [39].

A: application of load

B: yield point

C: necking or cold drawing

D: breaking load or breaking force

E: extension at break

The appearance of a permanent set is said to mark a ***yield point***, which indicates the upper limit of usefulness for any material. Most tension tests are continued until the fibre breaks. The load at that point is called the ***breaking load*** or ***breaking force***. The units for measuring breaking force include pounds, grams and newtons or millinewtons, abbreviated to lbf, gf, N and mN respectively.

To compare the breaking strengths of materials of varying sizes, it is necessary to express the breaking load in terms of the dimensions of the material being tested. The comparison is usually made based on the

cross-sectional area of the unstrained specimen, generally expressed as pound-force per square inch (lbf/psi), gram-force per square millimeter (gf/mm^2) or newton-force per square millimeter (N/mm^2).

Stress (σ) is the force applied to produce deformation in a unit area of a test specimen or is the ratio of the applied load to the original cross-sectional area expressed in lbs/in^2 or N/mm^2.

$$\sigma = \frac{F}{A} \qquad (5.1)$$

σ = stress (lbs/in^2, N/mm^2)
F = force or load (lbs, N)
A = cross-sectional area (in^2, mm^2)

Strain (ε) is the ratio of the elongation to the gauge length of the test specimen, or simply stated, the change in length per unit of the original length. It is expressed as a dimension ratio.

$$\varepsilon = \frac{L - L_0}{L_0} = \frac{\Delta L}{L_0} \qquad (5.2)$$

ε = strain
ΔL = elongation or change in length
= $L - L_0$
L_0 = original length
L = extended length

5.1.2 Modulus of Elasticity

Ultimate strength, elongation and ***elastic modulus (Young's modulus)*** can be obtained from the stress-strain curve (Figure 5.1). For determining Young's modulus (E), the slope of the initial tangent (i. e., the steepest portion of the curve) is measured.

When stress-strain curves are non-linear, the modulus of the polymer can be measured in four different ways, as shown in Figure 5.2.

5.1.3 Elongation [39]

In a breaking strength or tensile test, a fibre is extended until it breaks. The change in length due to stretching is referred to as ***elongation***. Elongation, or percent elongation, is defined as the ratio of the extension of a material to the length of the material prior to stretching. This relationship is shown by the following equation:

$$\% \text{ elongation} = \frac{(\text{extended length} - \text{original length})}{\text{original length}} \times 100 \qquad (5.3)$$

Traditional classifications can be used to describe the performance of a polymer under load, as shown in Figure 5.3.

Soft, Weak. These are polymers that show low modulus, low (or no) yield point and low elongation at break.

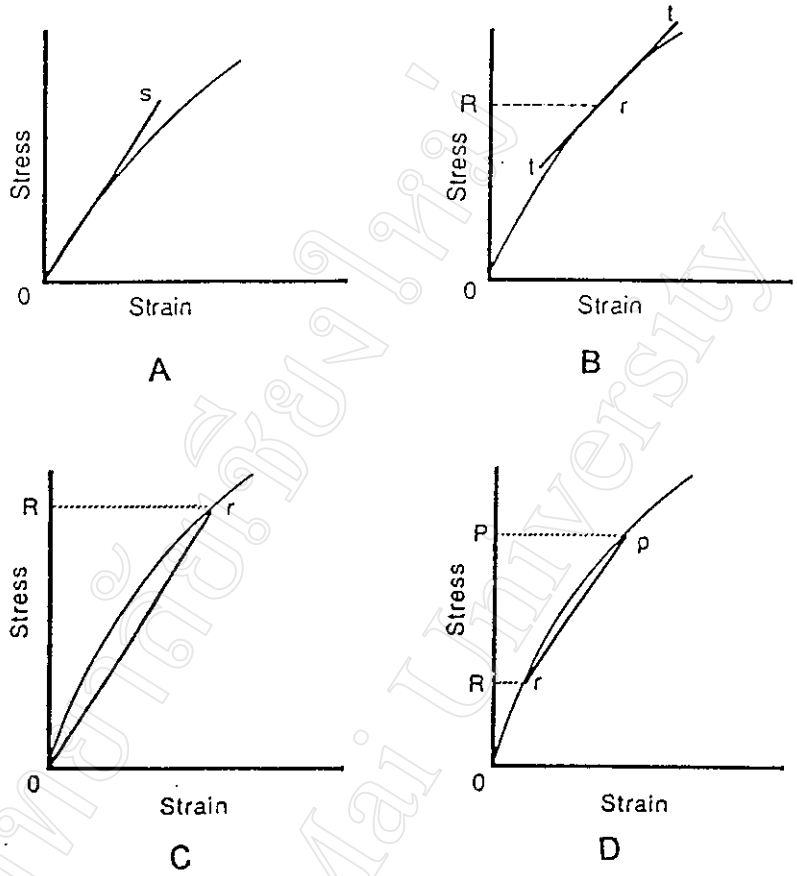

Figure 5.2: Four accepted methods of determining the elastic modulus from a non-linear stress-strain diagram [39].

(A) initial tangent modulus [s is the initial slope of curve]

(B) tangent modulus at stress R [t is tangent to curve]

(C) secant modulus between origin and stress R

(D) chord modulus between stresses R and P

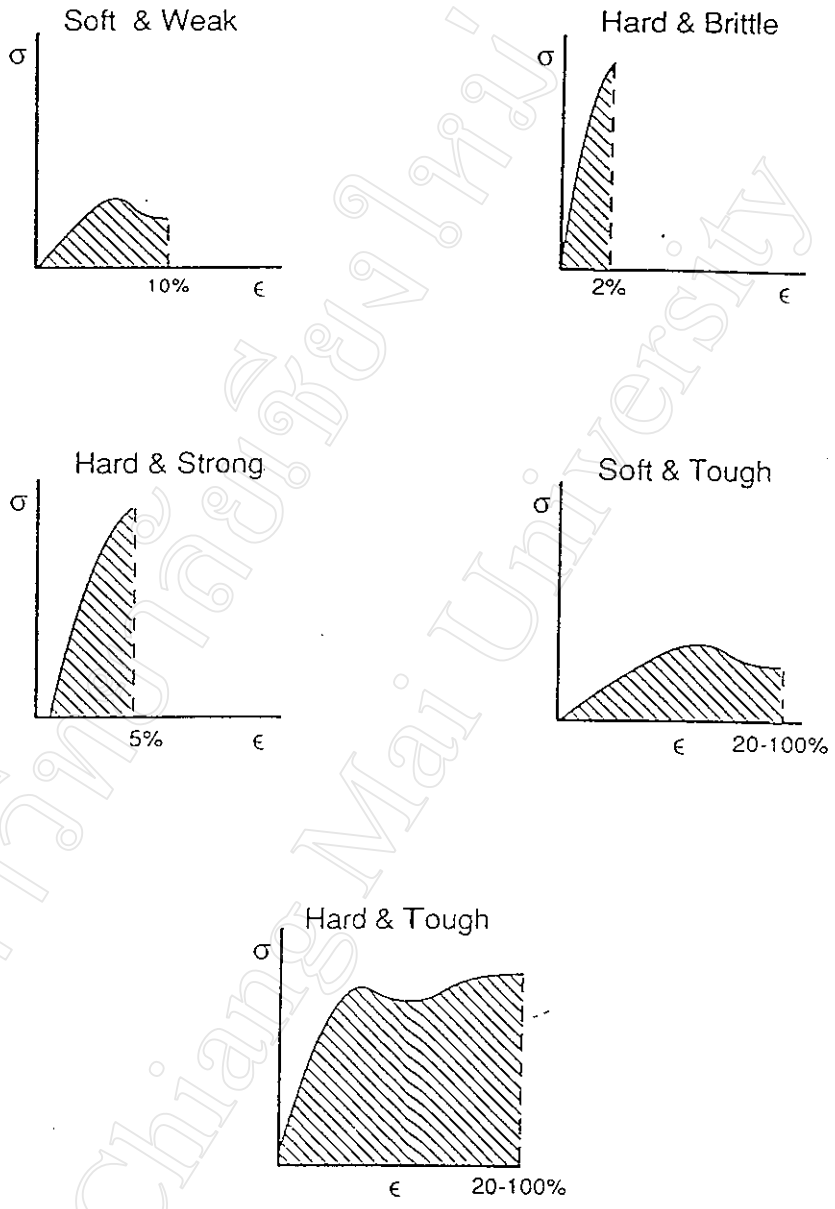

Figure 5.3: Classification of engineering stress-strain curves for polymers [39].

σ = applied stress

ε = resulting strain

Soft, Tough. These materials have low modulus, low yield point but very high elongation at break.

Hard, Brittle. These polymers have high modulus, no yield point and very low elongation at break.

Hard, Tough. These polymers have high modulus, high yield strength and relatively high elongation at break.

Hard, Strong. These materials have high modulus, high yield strength and relatively low elongation at break.

5.1.4 Tensile Test Results

The tensile tests in this project were performed on a Lloyds LRX+ Universal Mechanical Testing Machine, as shown in Figure 5.4. The dried fibres were cut into about 30 cm lengths and their diameters measured accurately with a micrometer. All tests (5 readings) were carried out with the monofilament sample wound once around two bollard grips (see Figure 5.5). An initial gauge length of 40 mm, a load cell of 100 N and a crosshead speed of 20 mm/min were used with the tests being carried out at room temperature (about 30°C). For the chitosan fibre produced at a ram speed of 12.9 mm/min and a take-up speed of 4 m/min with a diameter of 0.230 mm, the stress-strain diagram is shown in Figure 5.6. When compared with those in Figure 5.3, the shape of this stress-strain diagram suggests that the chitosan fibre can be classified as being somewhere in between a ***hard and brittle*** and a

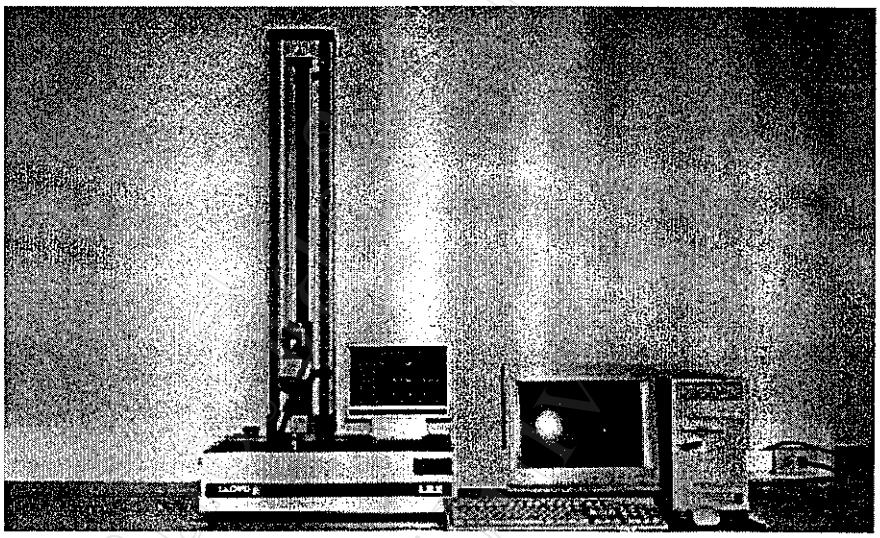

Figure 5.4: Photograph of the Lloyds LRX+ Universal Mechanical Testing Machine used for tensile testing.

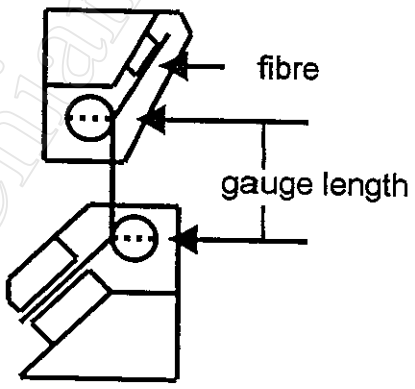

Figure 5.5: Diagram of the bollard grips used for tensile testing.

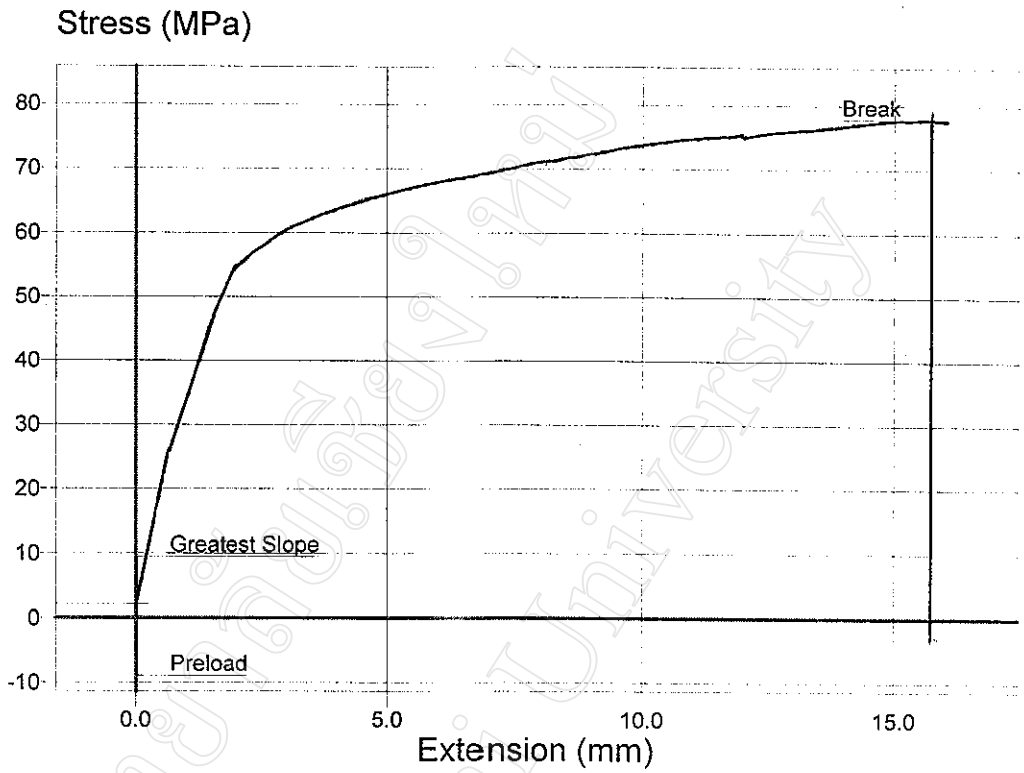

Figure 5.6: Stress-strain curve for the chitosan fibre produced at a ram speed of 12.9 mm/min and take-up speed of 4 m/min (diameter 0.230 mm).

Test Conditions

Sample Grips	:	Bollard-type
Initial Gauge Length	:	40 mm
Load Cell	:	100 N
Crosshead Speed	:	20 mm/min
Temperature/ Humidity	:	Ambient (approx. 30°C/ R.H. 70%)

hard and tough material. From Figure 5.6, it was found that the fibre had a stress and extension at break of 77.8 MPa and 15.7 mm (or 39.2%) respectively. The tensile test results for all of the samples prepared under the different processing conditions are compared in Table 5.1.

5.1.4.1 Effect of Ram Speed

From the results in Table 5.1, as the ram speed increased from 5-12.9 mm/min at a constant take-up speed of 2 m/min, the following effects on mechanical properties can be concluded:

(a) Although the load at break increased with ram speed due to the increased fibre diameter, the stress at break (i. e. tensile strength), which also takes into account the cross-sectional area, remained approximately constant. Tensile strength values of below 100 MPa are relatively low for monofilament fibres and reflect chitosan's rather poor mechanical strength.

(b) The extension or % strain at break showed no clear trend with increasing ram speed. Chitosan fibres are well known to be rather brittle in nature and liable to surface defects arising from the wet spinning process. Since the strain at break tends to be more sensitive to these factors than the stress at break, this may be the reason for the much wider variation in the strain results in Table 5.1.

(c) As would be expected, the stiffness values in Table 5.1 decrease with fibre diameter and ram speed. This is generally the case for monofilament fibres.

Thus, the effect of ram speed is mainly associated with the effect that the diameter of the fibre has on monofilament properties. The ram speed's main purpose therefore is to control the diameter of the fibre.

5.1.4.2 Effect of Take-up Speed

From Table 5.1, when the take-up speed was increased from 2-6 m/min at a constant ram speed of 12.9 mm/min, the following effects were observed:

(a) Increasing the take-up speed consistently decreases the fibre diameter and the load at break. However, the stress at break is again relatively constant (77-87 MPa) except for at the highest take-up speed (6 m/min) where the value suddenly increases by about 30% to 106 MPa. This could be the result of increased molecular orientation along the fibre axis brought about by drawing at the highest take-up speed.

(b) The extension / % strain at break results are inconclusive.

(c) The stiffness and modulus values at the highest take-up speed are only about a half of those at the lower speeds. This is most likely an effect of the reduced diameter of the fibre.

Thus, the main observed effect of the take-up speed in this work is to control the fibre diameter in combination with the ram speed. There is very little evidence of molecular orientation having been induced in the fibre during take-up speed except a slight indication perhaps at the highest speed. Due to

Table 5.1: Comparison of the mechanical properties of the chitosan fibres prepared under different processing conditions.

Ram Speed (mm/min)	Take-up Speed (m/min)	Average Diameter		Load At Break		Stress At Break		Extension At Break	
		(mm)	Variation (%)	(N)	Variation (%)	MPa	Variation (%)	(mm)	Variation (%)
5	1.5	0.238	± 2.2	3.4076	± 5.6	82.320	± 4.6	7.7759	± 8.9
	2	0.178	± 0.8	2.1678	± 1.4	86.508	± 1.5	11.6692	± 2.4
10	2	0.271	± 1.9	4.9088	± 6.0	85.103	± 2.1	5.2556	± 3.7
	3	0.224	± 1.4	3.7961	± 6.6	96.337	± 1.9	6.3980	± 3.4
12.9	2	0.309	± 1.0	7.0638	± 3.1	79.862	± 2.3	10.5206	± 2.5
	3	0.261	± 0.3	4.6692	± 4.6	87.079	± 2.4	10.5640	± 4.4
	4	0.230	± 0.2	3.5205	± 0.5	77.820	± 1.2	15.7010	± 1.5
	6	0.163	± 0.5	2.2134	± 2.1	105.979	± 2.1	9.9252	± 1.7

Notes:

(1) all values are the average of 5 readings

(2) the mechanical properties values are as a printed out on the sample test reports

(3) the stiffness indicated the modulus of sample

(4) the modulus values are obtained from the initial tangent to the curve (see Figure 5.2 (A) and Figure 5.6)

Table 5.1: Comparison of the mechanical properties of the chitosan fibres prepared under different processing conditions (continued).

Ram Speed (mm/min)	Take-up Speed (m/min)	% Strain At Break		Stiffness		Modulus	
			Variation (%)	(N/m)	Variation (%)	(MPa)	Variation (%)
5	1.5	19.440	± 2.3	2603.17	± 2.6	1776.7	± 2.5
	2	29.173	± 1.9	1565.60	± 1.8	2500.5	± 1.5
10	2	12.009	± 3.7	3206.00	± 2.1	2511.2	± 2.2
	3	15.871	± 2.6	2266.43	± 1.4	2317.8	± 2.2
12.9	2	26.296	± 2.7	3322.95	± 1.1	2581.0	± 1.4
	3	26.410	± 1.8	2734.33	± 0.9	2394.0	± 0.5
	4	39.255	± 1.1	2632.00	± 1.5	2221.9	± 1.9
	6	24.813	± 1.7	1302.18	± 1.1	1460.8	± 1.6

Notes:

(1) all values are the average of 5 readings

(2) the mechanical properties values are as a printed out on the sample test reports

(3) the stiffness indicated the modulus of sample

(4) the modulus values are obtained from the initial tangent to the curve (see Figure 5.2 (A) and Figure 5.6)

the very low tensile strength of the coagulated fibre, it is difficult to draw the wet fibre without breaking it. Molecular orientation through drawing is more likely to be achieved by hot drawing the dry fibre. This would be an interesting area for further study.

5.2 Scanning Electron Microscopy [40]

Optical and electron microscopy are commonly used to investigate the microstructural features of all types of material: metals, ceramics and polymers. Scanning electron microscopy is particularly useful because of the depth of focus that can be achieved, thus enabling 3-dimensional photographic images of the sample surface to be obtained.

5.2.1 Instrumentation

Scanning electron microscopy (SEM) is a technique which forms an image of a microscopic region of the specimen surface. An electron beam from 5 to 10 nm in diameter is scanned across the specimen. The interaction of the electron beam with the specimen produces a series of phenomena such as:

- back-scattering of electrons of high energy
- secondary electrons of low energy
- absorption of electrons; measurable as specimen current
- X-rays
- visible light (cathode luminescence)

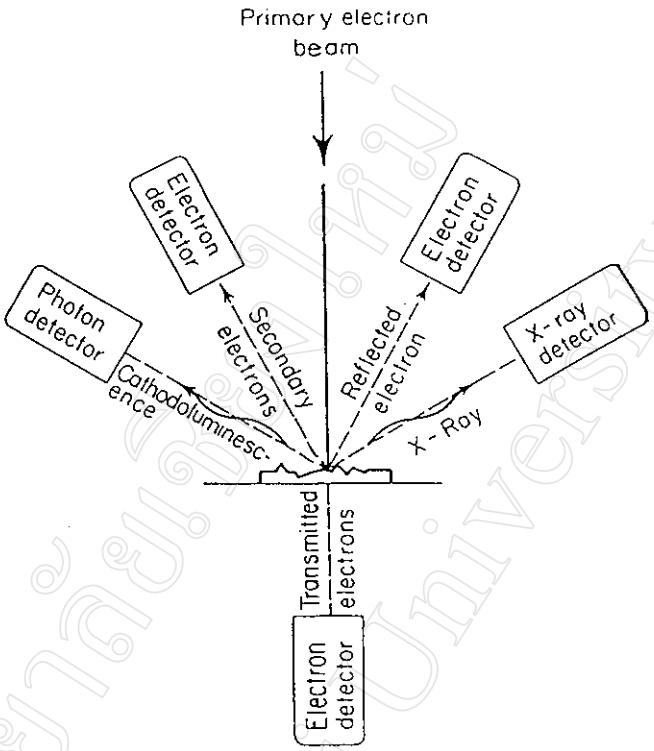

Figure 5.7: The range of information that can be generated in SEM by an electron beam striking the sample [40].

The electron gun comprises a tungsten filament which produces a flow of thermal electrons. These electrons are accelerated by applying a high voltage (1-30 kV) and the electron beam (see Figure 5.7) is focussed with the aid of a series of slits. The system of two-stage electromagnetic lenses is used to demagnify the electron beam diameter to 5-10 nm at the specimen. If the specimen is not a good electrical conductor, it should be coated with a thin layer (100-500 $\mathring{A}$) of conducting material (e.g., gold, silver, carbon or gold-palladium). This coating is carried out by placing the specimen in a high-vacuum evaporator and vaporizing a suitable metal held in a heated tungsten basket. Charging phenomena can be reduced by coating the specimen with organic antistatic agents from solution.

A series of detectors are employed to detect electrons, X-rays or cathodoluminescent light (photons) emitted from the sample. The signal from a detector is amplified and fed to a cathode ray tube, the beam of which is scanned in synchrony with the electron beam impinging upon the specimen. A correspondence between each scanned point at the specimen surface and a corresponding point on the cathode ray tube screen is thus established. The area upon the specimen surface is vary small in comparison with the corresponding area on the cathode ray tube screen. The magnification of the image on the screen (or photomicrograph) is the ratio of a distance on the screen to the corresponding distance on the specimen.

5.2.2 Experimental Results

In this research project, a Jeol 5410 Scanning Electron Microscope, was used to investigate the surface appearance of the chitosan fibres. For electrical conductivity, the fibres were gold-coated. From the SEM image in Figure 5.8, it can be seen that the surface of the fibre was mainly smooth and uniform but with a variety of localised surface irregularities distributed across it. These irregularities, which were too small to be seen by the naked eye or sensed by feel, are typical of wet-spun fibres and can be attributed to various factors such as:

(a) During the coagulation process, considerable shrinkage (volume reduction) takes place as the polymer precipitates out of solution in the spin dope. This shrinkage is particularly severe in the case of chitosan because the spin dope is so dilute (3% w/v). Consequently, considerable mass transfer has to take place as the fibre forms. This shrinkage effect,

particularly if uneven over the whole surface area, can cause surface irregularities.

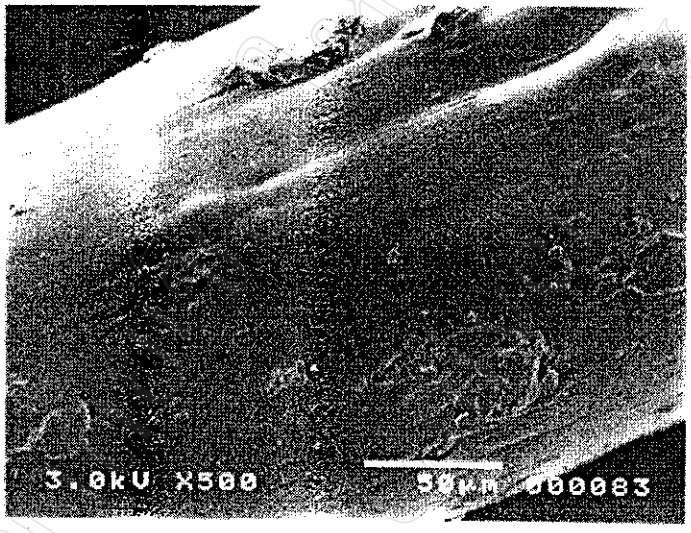

Figure 5.8: SEM photograph of dried chitosan fibre (magnification x 500). (Ram speed = 12.9 mm/min, take-up speed = 4 m/min)

(b) The instant that the spin dope contacts the coagulant, the polymer starts to precipitate and forms an outer gel layer which then affects the rate of diffusion of coagulant into the core of the fibre and diffusion out of water and acetic acid. These varying rates of diffusion and, hence, solidification during coagulation can also lead to internal stresses in the fibre which can lead to surface defects.

(c) Contact and possibly some degree of friction between the wet coagulated fibres and the rollers of the take-up unit may cause surface defects while the fibres are still soft. Compression during take-up may also occur leading to a non-circular cross-section.

(d) Drying of the washed fibres leads to more shrinkage and a change from a soft to a hard material. The resulting change in surface tension may also have an effect on the final surface topography.

(e) Finally, contamination by dust particles during the various stages of the spinning process cannot be discounted. Also, some of the surface irregularities in Figure 5.8 could have been caused during the sample preparation (e.g., gold coating) for SEM analysis and also by the electron beam during the analysis itself.

5.3 X-Ray Diffraction [22, 40]

The X-ray diffraction method is one of the most powerful techniques available for the examination of polymers in the solid state. In general, useful information can be obtained only if the polymer forms oriented fibres, is microcrystalline, or yields single crystals (polyethylene, crystalline globular proteins, viruses, etc). The following types of information can be obtained from X-ray diffraction measurements [40]:

(i) morphology of specimen (semi-crystalline or amorphous)
(ii) approximate amount of crystalline fraction
(iii) preferred orientation of crystallites
(iv) degree of alignment
(v) perfection of crystalline regions
(vi) translation period along the fibre axis

5.3.1 Instrumentation

An X-ray diffractometer (X-ray spectrometer) (Figure 5.9) is comprised of the following parts:

(i) An X-ray source which can be used in the form of a sealed X-ray tube or X-ray tubes with rotating anticathodes; the latest type of source produces higher intensity X-rays

(ii) Lenses and mirrors cannot be used with X-rays; a collimated beam can be obtained from an X-ray tube with an extended target by passage through a bundle of metal tubes (collimator) or, if collimation in one plane is required, through the space between a stack of parallel metal sheets (Soller slits) (Figure 5.9).

(iii) Crystal monochromators; a monochromatic beam can be obtained by reflecting (diffracting) the direct X-ray beam from the surface of a flat crystal (rock salt, fluoride, urea nitrate, or pentaerythritol) plate that has been cleaved or cut with its surface parallel to the diffracting planes.

(iv) A goniometer or specimen holder for mounting the specimen

(v) X-ray counters; there are three types of counters for X-ray intensity measurement

(vi) An amplifier, pulse-height analyzer, and recording system

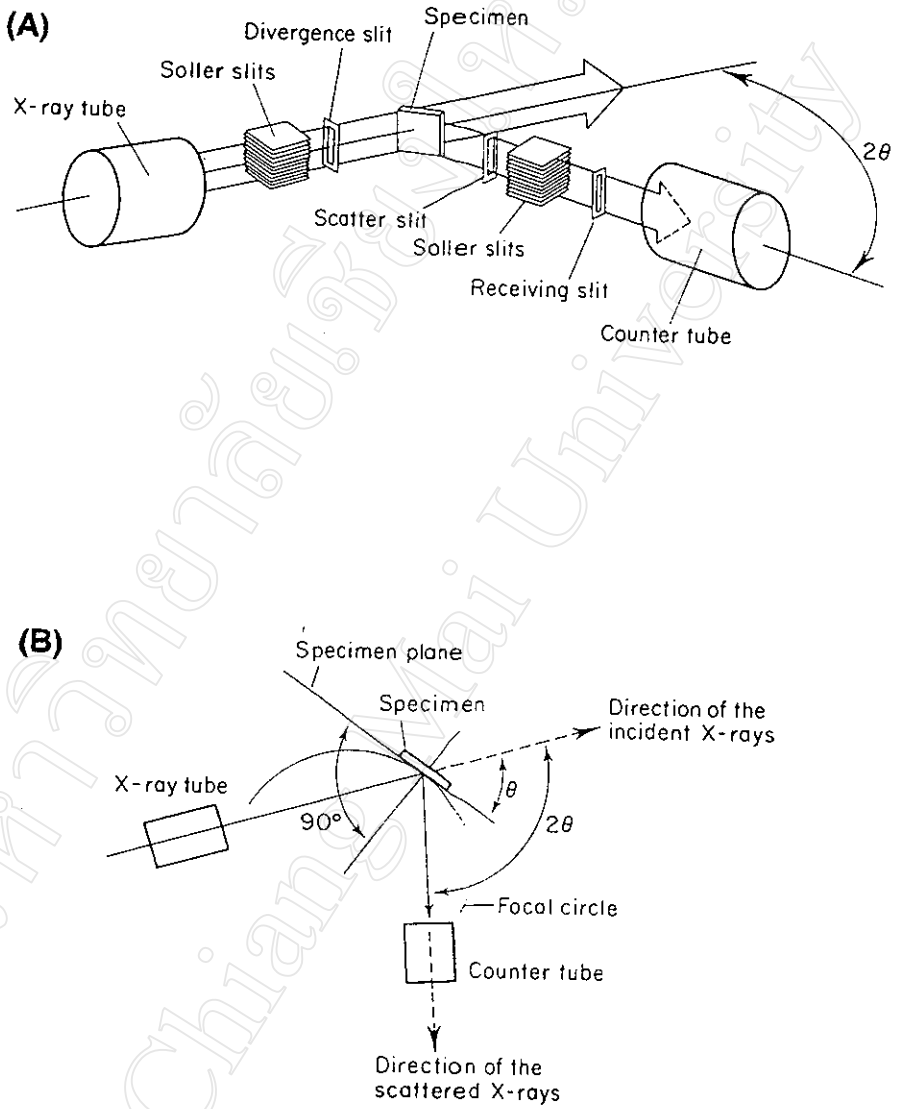

Figure 5.9: (A) Schematic representation and (B) geometry of an X-ray diffractometer [40].

5.3.2 Experimental Results

A Jeol X-Ray Diffractometer was the instrument used in this research project. The chitosan fibres produced at a ram speed of 12.9 mm/min and take-up speed of 4 m/mim were cut to about 1 inch lengths and then mounted parallel to one another in a small metal sample holder using tape and plasticene to hold the fibres in place, as shown in Figure 5.10.

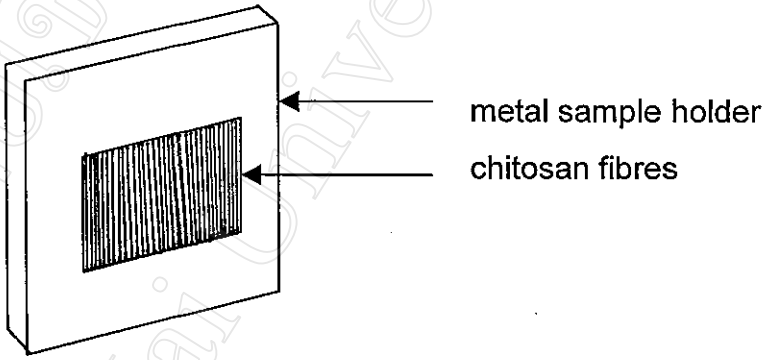

Figure 5.10: Chitosan fibre sample mounting for X-ray diffraction measurements.

Figures 5.11 and 5.12 show the X-ray diffraction patterns of the tape and plasticene alone (background) and with the chitosan fibres mounted in place respectively. In Figure 5.12, the sharp background peaks are easily distinguishable from the broad sample peaks. The fact that the sample peaks are so broad and diffuse is an indication that the degree of crystallinity of the fibres is quite low. Consequently, because the chains throughout the matrix are so disordered, when the incident X-rays impinge on the sample, they are diffracted in many different directions. Hence, the peaks obtained are broad.

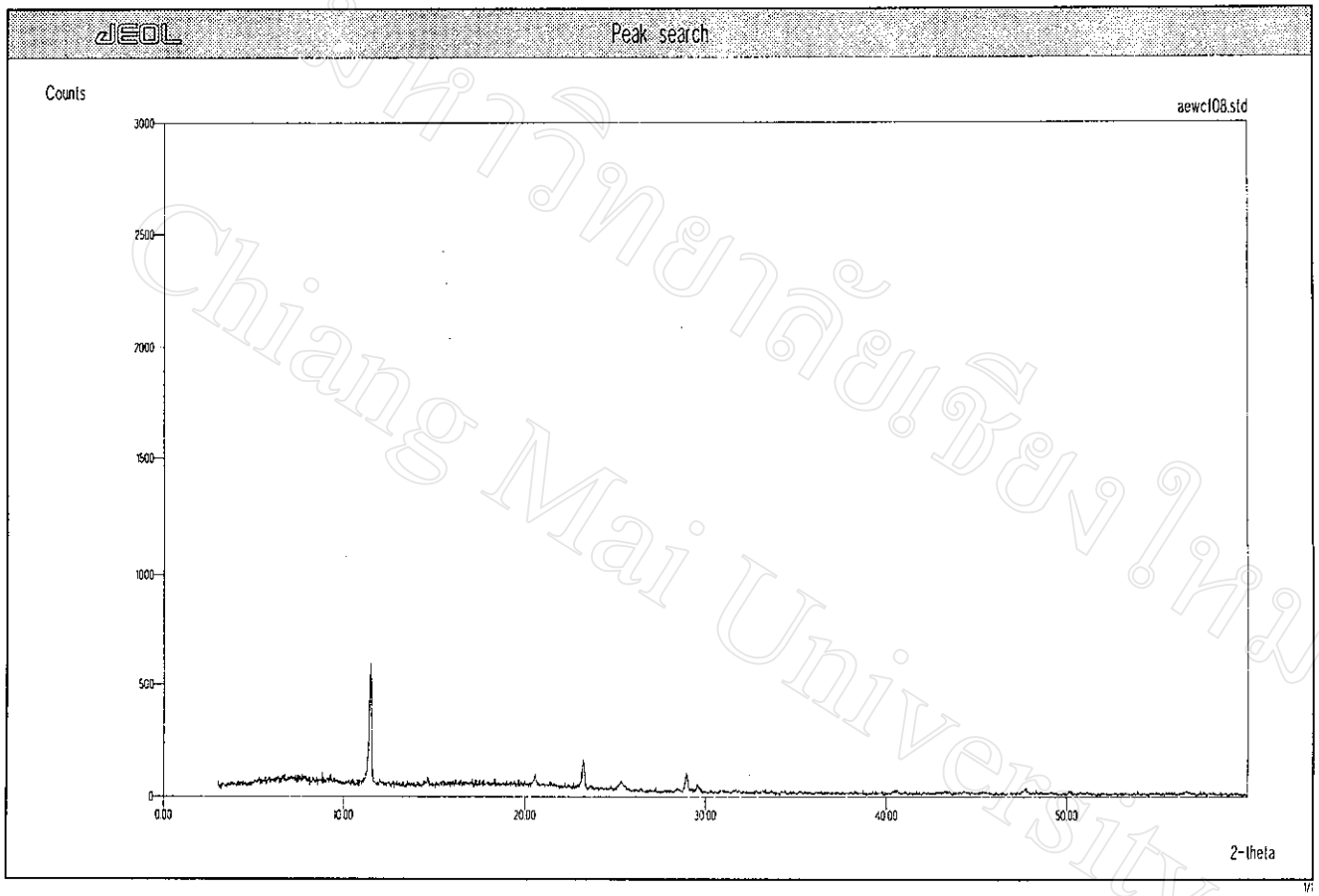

Figure 5.11: X-ray diffraction pattern of tape and plasticene (background).

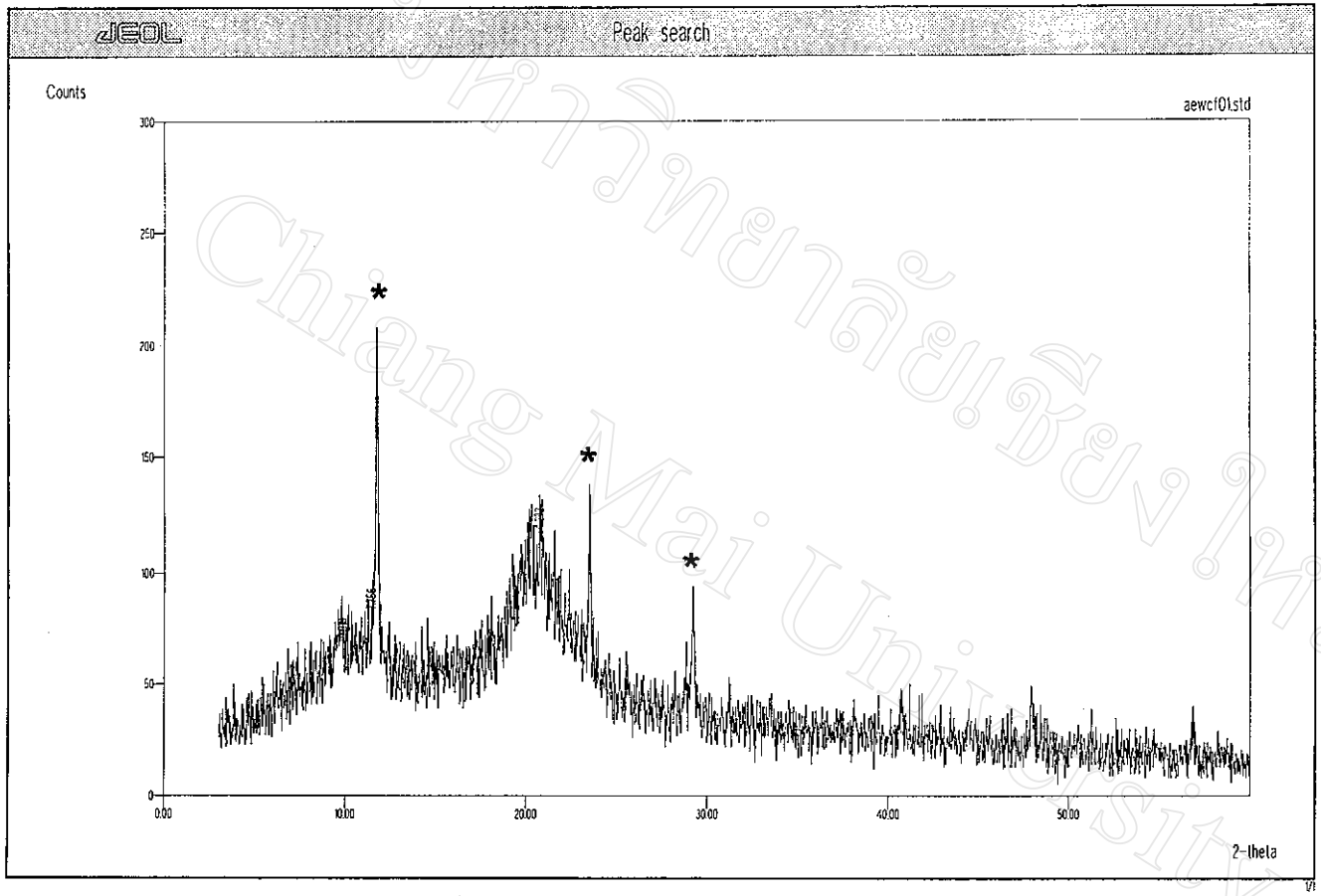

Figure 5.12: X-ray diffraction pattern of chitosan fibres. (Ram speed = 12.9 mm/min; take-up speed = 4 m/min)

* = background peaks

Differentiation between crystalline and amorphous scattering in a semi-crystalline polymer sample is shown in Figure 5.13. Normally, a line is drawn connecting the minima between the crystalline peaks. The scatter intensity above this line (I_c) is from the crystalline regions while the intensity below this line (I_a) is from the amorphous regions. The degree of crystallinity can then be estimated from:

$$\% \text{ crystallinity} = \frac{\text{area under crystalline scattering peaks}}{\text{total area (crystalline + amorphous scattering)}} \times 100\%$$

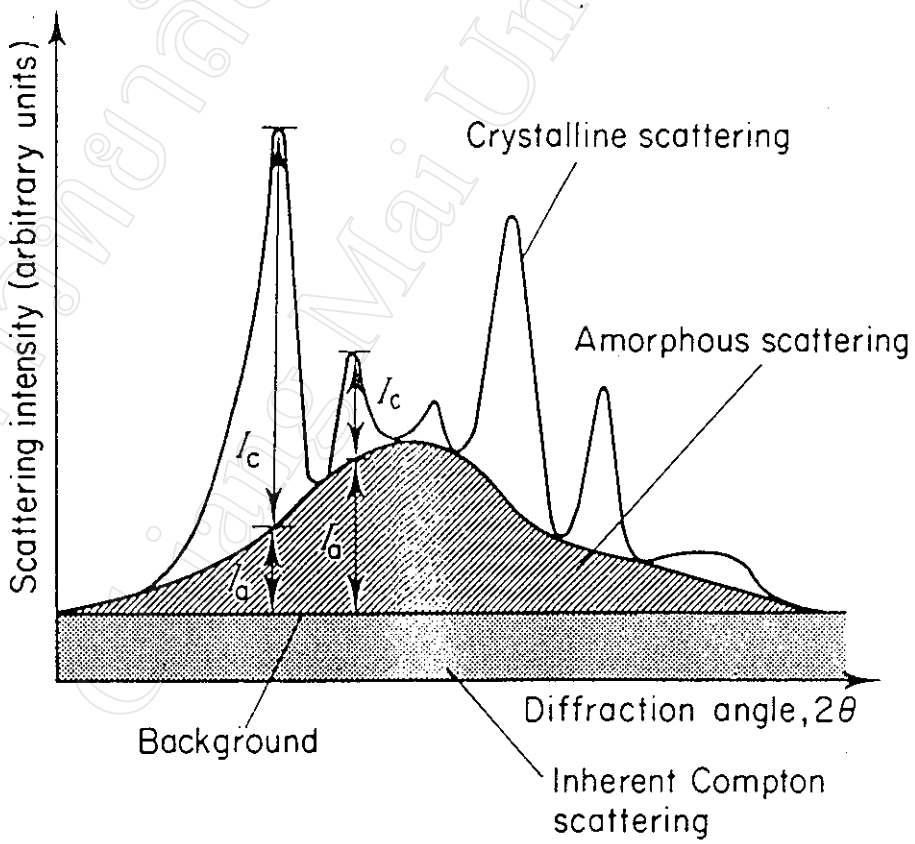

Figure 5.13: Differentiation between crystalline and amorphous scattering in the X-ray diffraction pattern of a semi-crystalline polymer [40].

However, in Figure 5.12, it is very difficult to differentiate accurately between the crystalline and amorphous scattering because of (a) the broad nature of the peaks and (b) the high baseline noise. The latter implies a weak signal from the sample which may have been partly due to the curved surfaces and spaces between the parallel fibres mounted in the sample holder. These would have combined to diminish the intensity of the scattered X-rays and, hence, the strength of the signal. Consequently, the fibres % crystallinity cannot be reliably estimated from the X-ray diffraction pattern in Figure 5.12.